Studies on Water-Swellable Elastomers. II. Thermal Properties and Crystalline Behavior of Amphiphilic Graft Copolymers with Poly(ethylene glycol) Side Chains

MIN LI,[1] ZHIYUAN XIE,[1] XINFANG CHEN,[1] SHUHUA LI[2]

[1] Department of Materials Science, Jilin University, Changchun 130023, People's Republic of China

[2] Changchun Institute of Applied Chemistry, Chinese Academy of Sciences, Changchun 130022, People's Republic of China

ABSTRACT: The thermal properties and crystalline structure of the amphiphilic graft copolymers CR-*g*-PEG600, CR-*g*-PEG2000, and CR-*g*-PEG6000 using chloroprene rubber (CR) as the hydrophobic backbone and poly(ethylene glycol)(PEG) with different molecular weights as the hydrophilic side chains were studied by DSC and WAXD. The results showed that a distinct phase-separated structure existed in CR-*g*-PEGs because of the incompatibility between the backbone segments and the side-chain segments. For all the polymers studied, T_{m2}, which is the melting point of PEG crystalline domains in CR-*g*-PEG, decreased compared to that of the corresponding pure PEG and varied little with PEG content. For CR-*g*-PEG600 and CR-*g*-PEG2000, T_{m1}, which is the melting point of the CR crystalline domains, increased with increasing PEG content when the PEG content was not high enough, and at constant PEG content, the longer were the PEG side chains the higher was the T_{m1}. The crystallite size L_{011} of CR in CR-*g*-PEGs increased compared to that of the pure CR and decreased with increasing PEG content. © 1997 John Wiley & Sons, Inc. J Appl Polym Sci **64:** 2441–2447, 1997

Key words: amphiphilic polymers; graft polymers; crystalline behavior; thermal properties; crystalline size; poly(ethylene glycol)

INTRODUCTION

Amphiphilic graft copolymers consisting of a hydrophobic backbone and hydrophilic branches have been the recent focus investigations because of their application as coatings, drug carriers, and polymer electrolytes.[1–3] The preparation and properties of amphiphilic graft copolymers have been the subject of recent investigations: Twaik et al.[4] Wesslen and Wesslen[5] and Iliyana et al.[6,7]

reported the grafting of poly(ethylene glycol) (PEG) and PEG monomethyl ethers (MPEG) onto different acrylic copolymers using transesterification or epoxide reactions. Direct anionic graft polymerization of ethylene oxide backbone polymers containing reactive functional groups[8] and the polymerization of PEG macromonomers[9] were also reported by the Wesslen group. Concerning the addition of hydrophilicity to rubber to prepare amphiphilic elastomers having applications not only as coating agents, packing materials, and water-leak sensors, but also for biomedical applications, only a few amphiphilic elastomers were reported, such as graft copolymers of polydimethylacrylamide-grafted natural rubber,[10] PEG-grafted-chlorosulfonated

$(x = 1, 2 \cdots \cdots ; \ y = 0, 1, 2 \cdots \cdots ; \ z = 1, 2 \cdots \cdots)$
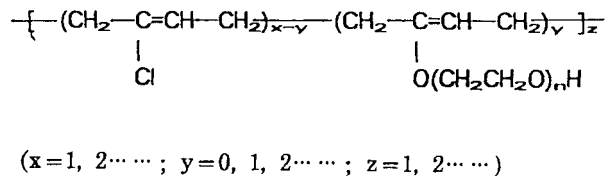
Figure 1   The molecular structure of CR-*g*-PEG.

polyethylene,[11] and PEG-grafted-butyl rubber.[12–14] At present, studies on amphiphilic graft copolymers were focused mostly on the preparation, while studies on the condensed structure and physical properties are few. Recently, we reported the synthesis and characterization of chloroprene rubber-*graft*-PEG (CR-*g*-PEG) and this article deals with the crystalline structure and thermal properties of CR-*g*-PEG. The effect of the length of the grafts and the distribution of the grafts along the CR backbone (σ) on the melting point, crystallinity, and the crystallite size are discussed.

EXPERIMENTAL

Synthesis of CR-*g*-PEG

The synthesis of CR-*g*-PEG was based on the reaction between the sodium salt of PEG and chlorine in CR. The details of the synthetic procedure were described in our previous article.[15] The molecular structure of CR-*g*-PEG is given in Figure 1.

Calculation of Molecular Parameters of CR-*g*-PEG

The molecular parameters of CR-*g*-PEG were determined according to the following equations:

$$P_A = \frac{m_{C1} + m_1 \cdot W_{C1}}{(M_{n2} - m_{C1}) \cdot W_{C1} + m_{C1}} \quad (1)$$

$$\sigma = P_A P_{n1} \quad (2)$$

PEG content (%)

$$= \frac{P_A \cdot M_{n2}}{P_A(M_{n2} + m_1') + (1 - P_A)m_1} \quad (3)$$

$$m_1' = m_1 - m_H$$

where P_A is the degree of the graft reaction; m_{C1}, the atomic weight of chlorine; m_1, the molecular weight of the monomeric unit of CR; W_{C1}, the weight percent of chlorine in graft copolymers de-

termined by elemental analysis; M_{n2}, the molecular weight of the PEG side chains; P_{n1}, the number-average degree of polymerization of CR; and σ, the average number of PEG grafts per CR backbone. For calculations, $M_{n1} = 6.9143 \times 10^4$ and $M_{n2} = 600, 2000,$ and 6000, respectively.

Calculation of Crystallite Size

The crystallite size was calculated using the Scherrer equation[16]:

$$L_{hkl} = 57.3 \, K\lambda/\beta \cos \theta$$

where $L_{hkl}(\text{Å})$ is the mean dimension of crystallites perpendicular to planes hkl; K, the shape factor ($K = 0.9$); λ, the X-ray wavelength; and 2θ, the Bragg angle. $\beta^2 = B^2 - b_0^2$, and B is measured half-width of the experimental profile (degree); β, the pure broadening profile (degree); and b_0, the instrumental broadening factor (degree), which is $0.15°$ in our calculations.

Measurement

Differential scanning calorimetry (DSC) analysis was carried out on a Perkin-Elmer DSC-2C in N_2, and the scanning rate of the temperature was 10 K/min. The sample loaded was ca. 10 mg and the temperature range was 240–373 K.

A wide-angle X-ray diffraction (WAXD) measurement was performed on a Rigaku D/MAX-rA (Rigaku Co., Japan) X-ray diffractometer with nickel-filtered CuK_α radiation at room temperature. The thickness of the sample films was ca. 0.5 mm. Elemental analysis of chlorine in CR-*g*-PEGs was done in an analytical laboratory of the Changchun Institute of Applied Chemistry, Chinese Academy of Sciences, China.

RESULTS AND DISCUSSION

Thermal Properties of CR-*g*-PEG

Hydrophobic segments and hydrophilic segments of an amphiphilic polymer are generally incompatible with each other, forming a phase-separated structure. The characteristics of the structure affect not only the performances but also the functions of the materials. Therefore, it is very important to study the properties and the structures of CR-*g*-PEG.
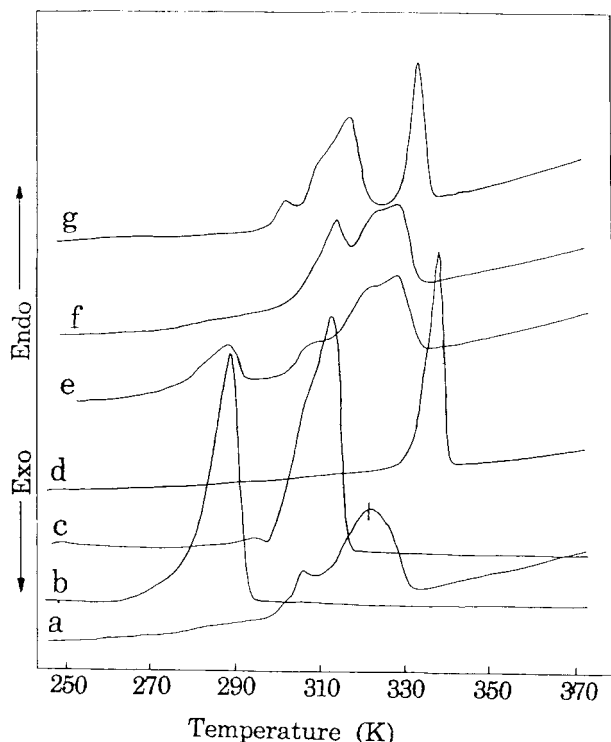
Figure 2 DSC curves of (a) CR, (b) PEG600, (c) PEG2000, (d) PEG6000, (e) CR-*g*-PEG600 (PEG content: 17.26%), (f) CR-*g*-PEG2000 (PEG content: 8.40%), and (g) CR-*g*-PEG6000 (PEG content: 35.60%).

DSC analysis was used to evaluate the miscibility of the multicomponent systems of CR-*g*-PEG. DSC curves of CR-*g*-PEG with different molecular weights of PEG and different σ are shown in Figure 2. It can be seen that the DSC curves of CR-*g*-PEGs show two melting peaks corresponding to the melting of CR crystals (T_{m1}) and PEG crystals (T_{m2}), respectively. Compared to the corresponding homopolymers, the melting points (T_{m1} and T_{m2}) of the graft copolymers shifted to high or low temperature due to the interaction between the backbone segments and the side-chain segments. The coexistence of the melting points of the corresponding homopolymers in the graft copolymers indicated that the hydrophobic segments (CR) and the hydrophilic segments (PEG) are incompatible with each other and thus resulted in a phase-separated structure in CR-*g*-PEG.

The T_{m1}, T_{m2}, and the crystallinity of CR domains (ΔH_{m1}) of the graft copolymers are listed in Table I. It can be seen that the T_{m1} of CR-*g*-PEG600 was lower than that of the pure CR and

increased with increasing PEG content when the PEG600 content was lower than 22%. No endotherm peak can be detected in the course of heating for sample no. 22 in which the PEG content was 37.4%. The T_{m1} of sample no. 22 after being annealed was 307.4 K, which was 13 K lower than that of the pure CR. For the CR-*g*-PEG2000 studied, T_{m1} was higher than that of pure CR and increased with increasing PEG2000 content. The T_{m2} of the graft copolymers with PEG600 and PEG2000 as side chains was lower than that of pure PEG and changed little with PEG content, while for CR-*g*-PEG6000, T_{m2} and T_{m1} were both lower than those of the corresponding homopolymers CR and PEG.

From the above analysis, it can be inferred that the CR crystallized first in the course of the melt crystallization of CR-*g*-PEG and the influence of the PEG side chain on the melting temperature of CR in CR-*g*-PEG resulted in two aspects: on the one hand, the steric hindrance of PEG constrains the regular arrangement of the CR segment, which in effect, causes T_{m1} to decrease; on the other hand, the molecular arrangement of CR in the graft copolymers can be stabilized by the intermolecular interaction between the PEG terminal groups (— OH), which, in effect, causes T_{m1} to increase.

The above two opposite effects of the PEG side chain affected the T_{m1} of CR-*g*-PEG: When the PEG content was not high enough, the latter case was dominant, so T_{m1} was higher than that of pure CR and increased with PEG content, while for graft copolymers with a high enough PEG content (e.g., sample no. 22), the former case was dominant. T_{m1} decreased because of the larger steric hindrance of PEG to the regular arrangement of the CR segment, and T_{m2} was lower than that of the homopolymer PEG600 and PEG2000 due to the constraints of the CR crystals to the PEG's regular arrangement. But for the studied CR-*g*-PEG6000, PEG6000 crystallizes first in the course of melt crystallization; therefore, T_{m1} and T_{m2} decreased compared to the pure component of CR and PEG6000. Also, it can be seen that the longer the side chain the higher was the T_{m1} for the graft copolymers at constant PEG content. This phenomenon can be explained by that the steric hindrance was lower in the graft copolymers with longer side chains in the case of the same PEG content. The ΔH_{m1} of CR-*g*-PEG with different molecular weights of PEG are listed in

Table I   Effect of σ and PEG Content on the Thermal Properties of CR-*g*-PEG

Sample No.	M_n of PEG	PEG (Wt %)	σ	T_{m2} (K)	T_{m1} (K)	ΔH_{m2} (J/g)	ΔH_{m1} (J/g)	$\Delta H_{m1'}$ (J/g)
CR	—	—	—	—	321.1	—	19.06	—
PEG600	600	100	—	289.4	—	101.8	—	—
2	600	5.04	6.09	282.2	322.9	—	14.7	15.4
11	600	8.96	11.27	280.1	325.7	—	27.4	30.1
21	600	17.26	23.74	288.4	328.1	6.35	25.3	30.6
6	600	21.11	30.36	—	328.7	—	26.1	33.1
22	600	37.40	66.42	—	—	—	—	—
22′	600	37.40	66.42	281.4	307.9	—	8.84	14.1
PEG2000	2000	100	—	317.1	—	150.8	—	—
8	2000	5.88	2.16	312.7	324.9	—	20.8	22.1
23	2000	8.40	3.16	313.8	327.7	—	20.3	22.2
24	2000	21.34	9.33	313.2	329.6	—	20.8	26.4
PEG6000	6000	100	—	338.6	—	185.7	—	—
25	6000	35.62	6.35	334.7	318.0	20.6	10.7	16.6

$\Delta H_{m1} = \Delta H_{m1'}$ wt % of CR in the copolymers. Sample no. 22′ was obtained by annealing Sample 22 at 43°C for 2 h.

Table I. It can be seen that ΔH_{m1}, which is the melting enthalpy change of CR in the graft copolymer, increased with increasing PEG content when the PEG content was not high enough, indicating that the crystallinity of CR in the graft copolymers increased because of the introduction of PEG side chains. The melting enthalpy change (ΔH_{m1}) of CR in the graft copolymers with shorter PEG side chains (no. 6) was larger than that of the graft copolymers with longer ones (no. 24), indicating that CR segments in the graft copolymers with shorter side chains are liable to aggregate to form a crystalline region, although the steric hindrance was large and the crystalline domain can be stabilized by PEG side chains because of the polar interaction between the PEG terminal groups.

WAXD Patterns of CR, PEG, and CR-*g*-PEG

The WAXD patterns of the homopolymer PEG and CR are shown in Figure 3. It can be seen that CR was a semicrystalline polymer with three major peaks at 20.1°, 21.9°, and 26.6°, respectively. WAXD studies on CR showed that the unit cell of CR was orthorhombic[17]: $a = 0.88$ nm, $b = 1.02$ nm, and $c = 0.48$ nm. According to the unit cell parameters, the two major peaks at 20.1° and 21.9° corresponded to planes 011

and 210, respectively. The amorphous halo of CR was centered at 20.2°.

The two major peaks of PEG with a high enough molecular weight were 19.3° and 23.4°, respectively. The two major peaks corresponded to planes 120 and 113/032, respectively, according to the unit cell parameters of PEG[18] with $a = 0.796$ nm, $b = 1.311$ nm, $c = 1.939$ nm, and $\beta = 124°\ 48'$. The amorphous halo of PEG was in the vicinity of 21.2°.

Crystalline Structure of CR-*g*-PEG

WAXD patterns of CR-*g*-PEG6000 are shown in Figure 3. It can be seen that the position of the diffraction peaks of CR and PEG in the graft copolymers did not change, indicating that the unit cell parameters of CR and PEG in the graft copolymers did not change although the relative intensity of the diffraction peaks changed and, also, that CR and PEG crystallized separately. Because of the low melting temperature of PEG600 and the low relative intensity of the diffraction peaks of PEG2000, no diffraction peaks of PEG can be detected in the WAXD patterns of CR-*g*-PEG600 and CR-*g*-PEG2000. To study the effect of PEG side chains on the crystalline structure of CR-*g*-PEG, the Scherrer equation was used to calcu-
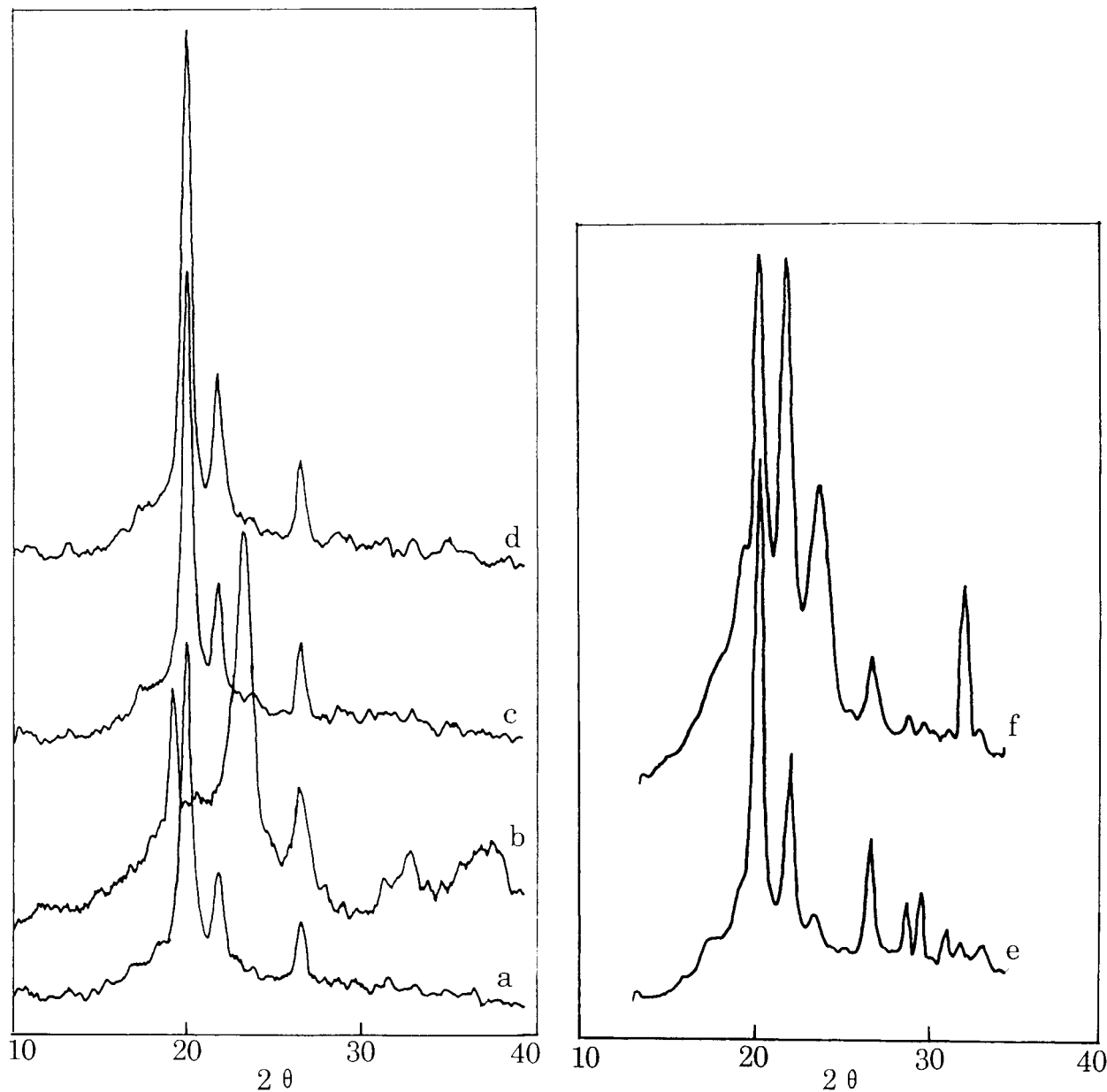
Figure 3 WAXD spectra of (a) CR, (b) PEG 2000, (c) CR-g-PEG600 (PEG content: 21.11%), (d) CR-g-PEG2000 (PEG content: 21.34%), (e) CR-g-PEG6000 (PEG content: 35.60%), and (f) CR-g-PEG6000 (PEG content: 51.33%).

late the crystallite sizes of the graft copolymers. The results of the calculated crystallite size are shown in Table II. The crystallite size L_{011} of CR in the graft copolymers was larger than that of pure CR, ranging from 12.7 to 16.1 nm, and L_{011} decreased with increasing σ of the graft copolymer, the phenomenon of which re-

flected the inhibition of the PEG side chains to crystallize CR along the normal direction of plane 011. The longer the PEG side chains, the larger the L_{011} became at the constant PEG content. The L_{011} of CR in the graft copolymers increased because of the thermal annealing of the graft copolymers, which meant that the

Table II   Crystallite Size of the Graft Copolymers (CR-*g*-PEG)

Sample No.	M_n of PEG	PEG (Wt %)	σ	hkl	2θ (°)	$\cos\theta$	B (°)	β (°)	L_{hkl} (nm)
CR	0	0	—	011	20.053	0.9847	0.6532	0.6357	12.7
				210	21.878	0.9818	0.6793	0.6625	12.2
PEG	2000	100	—	210	19.295	0.9859	0.4180	0.3920	20.6
				113/032	23.402	0.9792	1.0450	1.0342	7.85
25	6000	35.62	6.35	011	20.071	0.9847	0.5225	0.5005	16.1
				210	21.894	0.9818	0.5225	0.5005	16.2
				113/032	23.465	0.9791	1.0450	1.0342	7.85
26	6000	51.31	12.07	011	19.887	0.9850	0.5774	0.5376	14.5
				210	21.432	0.9826	0.7315	0.7160	8.24
				113/032	23.431	0.9792	1.0450	1.0342	7.85
24	2000	21.34	9.33	011	20.057	0.9848	0.6064	0.5878	13.7
				210	21.856	0.9819	0.5225	0.5005	16.2
6	600	21.11	30.36	011	19.937	0.9849	0.5486	0.5277	15.3
				210	21.760	0.9818	0.5225	0.5005	16.2
22	600	37.40	66.42	011	20.071	0.9847	0.6532	0.6357	12.7
				210	21.842	0.9819	0.5225	0.5005	16.2
22′	600	37.40	66.42	011	20.071	0.9847	0.5748	0.5549	14.6
				210	21.801	0.9819	0.6532	0.6357	12.7
22″	600	37.40	66.42	011	20.061	0.9847	0.5225	0.5005	16.1
				210	21.750	0.9819	0.7838	0.7693	10.5

Sample 22′ and Sample 22″ are obtained by annealing Sample 22 at 43 and −10°C for 2 h, respectively.

thermal annealing was favorable to the growth of the crystallite along the normal direction of plane 011.

CONCLUSIONS

A distinct phase-separated structure existed in CR-*g*-PEG because of the incompatibility of the CR backbone and PEG side chains. DSC studies on the thermal properties of CR-*g*-PEG showed that the introduction of PEG side chains can stimulate the crystallization of CR in a certain range of PEG content and the two opposite effects of PEG coaffected the melting points of the graft copolymers. The crystallite size L_{011} of CR in the graft copolymers was larger than that of pure CR and decreased with increasing PEG content. Thermal annealing was favorable to the growth of the crystallite of CR along the normal direction of plane 011.

REFERENCES

1. J. Chuji, T. Shishino, Y. Tsukahara, and Y. Yamashita, *Polym. J.,* **17,** 133 (1985).
2. M. Akashi, M. Wada, S. Yanase, and N. Miyauchi, *J. Polym. Sci. Polym. Lett. Ed.,* **27,** 377 (1989).
3. P. V. Wright, *J. Macromol. Sci.-Chem. A,* **26,** 519 (1989).
4. M. A. Twaik, M. Tahan, and A. Zilkha, *J. Polym. Sci. A-1,* **7,** 2469 (1969).
5. B. Wesslen, and K. B. Wesslen, *J. Polym. Sci. Part A Polym. Chem.,* **27,** 3915 (1989).
6. I. V. Berlinova, A. Amazil, S. Tsvetkova, and I. M. Panayotov, *J. Polym. Sci. Part A Polym. Chem.,* **32,** 1523 (1994).
7. I. V. Berlinova, A. Amazil, S. Tsvetkova, and I. M.

Panayotov, *J. Macromol. Sci. Pure Appl. Chem. A,* **29**(11), 975 (1992).

8. G. Bo, B. Wesslen, and K. B. Wesslen, *J. Polym. Sci. Part A Polym. Chem.,* **30,** 1799 (1992).

9. P. Jannasch, and B. Wesslen, *J. Polym. Sci. Part A Polym. Chem.,* **31,** 1519 (1993).

10. M. T. Razzak, K. Otsuhara, Y. Tabata, F. Ohashi, and A. Takeuchi, *J. Appl. Polym. Sci.,* **36,** 645 (1988).

11. M. Watanabe, A. Sekiya, H. Ishida, M. Tamura, S. Kamagami, and I. Yamaji, *Nihon Gomu Kyokai-Shi (J. Rubb. Soc. Jpn.),* **62,** 235 (1989).

12. Y. Ikeda, K. Kodama, K. Kajiwara, and S. Kohjiya, *J. Polym. Sci. Part B Polym. Phys.,* **33,** 387 (1995).

13. S. Yamashita, in *Frontiers of Macromolecular Science,* T. Saegusa, T. Higashimura, and A. Abe, Eds., Lackwell, Oxford, 1989, p. 201.

14. S. Yamashita, K. Kodama, Y. Ikeda, and S. Kohjiya, *J. Polym. Sci. Part A Polym. Chem.,* **31,** 2437 (1993).

15. Z. Y. Xie, M. Li, X. F. Chen, H. Z. Hu, and S. H. Li, *J. Appl. Polym. Sci.,* **61,** 495 (1996).

16. L. E. Alexander, *X-ray Diffraction Methods in Polymer Science,* Wiley-Interscience, New York, 1969, Chap. 7.

17. C. W. Bunn, *Proc. R. Soc. Lond. Ser. A.,* **180,** 40 (1942).

18. F. E. Bailey and J. V. Koleske, *Poly(ethylene oxide),* Academic Press, New York, 1976, p. 105.